UNIVERSITY *of* York

This is a repository copy of *Assessing vermetid reefs as indicators of past sea levels in the Mediterranean*.

White Rose Research Online URL for this paper:
https://eprints.whiterose.ac.uk/170425/

Version: Accepted Version

White Rose
university consortium
Universities of Leeds, Sheffield & York

eprints@whiterose.ac.uk
https://eprints.whiterose.ac.uk/

Assessing vermetid reefs as indicators of past sea levels in the Mediterranean

[1]Sisma-Ventura, G., [2]Antonioli F., [3]Silenzi, S., [3]Devoti, S., [4]Montagna, P., [5]Chemello, R., [6]Shemesh, A., [6]Yam, R., [7]Gehrels, R.,[8]Dean, S., [1]Rilov, G., [9]Sivan, D

[1]Israel Oceanographic and Limnological Research (IOLR), Haifa, Israel; [2]ENEA Casaccia, Roma, Italy; [3]ISPRA, Roma, Italy; [4]ISP, CNR, Bologna, Italy; [5]Department of Earth and Marine Sciences, Section of Ecology, University of Palermo, Italy; [6]Department of Earth and Planetary Sciences, Weizmann Institute of Science, Rehovot, Israel; [7]Department of Environment & Geography, University of York, UK; [8]Department of Earth Sciences, University of Pisa, Italy; [9]Department of Maritime Civilizations, L. Charney School of Marine Sciences, University of Haifa, Israel

Abstract

The endemic Mediterranean reef building vermetid gastropods *Dendropoma petraeum* complex (*Dendropoma* spp) and *Vermetus triquetrus* develop bio-constructions (rims) on rocky shorelines at about Mean Sea Level (MSL) and are therefore commonly used as relative sea-level (RSL) markers. In this study, we use elevations and age data of vermetid reefs to (1) re-assess the vertical uncertainties of these biological RSL indicators, and (2) evaluate the vertical growth rates along a Mediterranean east-west transect, in attempt to explain the differences found in both growth rates and uncertainties. In Israel, Differential Global Positioning System (DGPS) and laser measurements relative to the local datum show that the reef surfaces mainly occupy the upper intertidal zone with variations in elevation from +0.51±0.07 m to +0.13±0.05 m along the coast. However, in specific sites the vertical uncertainty exceeds the tidal range. In some places the local vermetid species *D. anguliferum* and *V. triquetrus* appear to alternate along the vertical rim profiles. This study documents a spatial variability of vertical growth

rates, ranging from ~1 mm yr^{-1} in Israel and Crete, to ~0.1-0.2 mm yr^{-1} in NW Sicily and Spain. The order of magnitude of the difference in growth rates correlates with the east-west spatial thermal gradient of Sea-Surface Temperature (SST). Preferential skeleton deposition of *D. petraeum* and *V. triquetrus* measured by growth axis $\delta^{18}O$ analysis shows that most calcification occurs at SST above the mean annual value. These findings indicate that vermetid reefs are a site-specific RSL indicator, displaying various vertical uncertainties and inner-structure complexities. Local data on the indicative range of vermetids are required when reconstructing relative sea-level changes using fossil vermetids.

1. Introduction

Given its mid-latitude position and very small tidal range, the Mediterranean is potentially a suitable area to reconstruct past sea-level changes with high precision and accuracy (e.g., Sivan et al., 2001; 2004; Milne and Mitrovica, 2008). One of the tools used in the Mediterranean to reconstruct past relative sea-level (RSL) change is based on endemic bio-markers: the coralline rhodophyte, *Lithophyllum byssoides* (Lamarck) rims inhabiting the western and northern Mediterranean, and the sessile, aggregative, tube-building gastropods of the genus *Dendropoma* (Laborel, 1986; Laborel et al., 1994; Laborel and Laborel-Deguen, 1996; Faivre et al., 2013). *Dendropoma* forms rims at the edge of vermetid reef platforms inhabiting the south and east Mediterranean (Safriel, 1975a,b; Antonioli et al., 1999; Silenzi et al., 2004; Sivan et al., 2010). Both species inhabit the intertidal rocky shorelines close to the Mean Sea Level (MSL). *Lithophyllum* rims have been also described as sea-level bio-markers (Laborel and Laborel-Deguen, 1996) along the coasts of southern France (Laborel et al., 1994; Lambeck and Purcell, 2005) and the Adriatic coast of Croatia (Faivre et al., 2013; 2019). In the eastern Mediterranean,

Dendropoma anguliferum (a Levant endemic formerly known as *D. petraeum*, Templado et al, 2016) rims studied by Safriel, (1975a,b) were used for determining vertical tectonic relative land movements (e.g., Pirazzoli et al., 1991; 1994; Morhange et al., 2006; Sivan et al., 2010) and late Holocene relative sea-level changes (Morhange et al., 2015; Dean et al., 2019).

Based on radiocarbon dating of *Dendropoma cristatum* in cores along the northern Sicilian coast vertical rim growth during the last 400 years was suggested to be a function of RSL rise (Antonioli et al., 1999; Silenzi et al., 2004). Moreover, vertical growth of *D. anguliferum* during the last millennium was measured in rims along the Israeli coast and used for paleoceanographic reconstructions (Sisma-Ventura et al., 2009; 2014, Bialik and Sisma-Ventura, 2016). These studies have shown that fast growing *Dendropoma* spp. rims provide a high-resolution archive of past sea-surface conditions. For example, a sea-level low-stand was reconstructed during the Crusader period by Dean et al. (2019), using down-core ^{14}C data of *Dendropoma* reefs from Israel in combination with archaeological sea-level index points. In this region, *Dendropoma* reefs have high vertical growth rates (~ 1.0 mm yr^{-1}) (Sisma-Ventura et al., 2014). However, a recent study by Amitai et al. (2020) reported variable vertical rim growth rates across the Mediterranean, suggesting that reef growth rates may vary regionally. Slow growing reefs are less likely to record abrupt changes in RSL. Regional variability is also apparent in the east–west genetic differentiation of the Mediterranean *Dendropoma petraeum*, comprising a complex of at least four cryptic species with non-overlapping ranges (Templado et al., 2016) that has resulted from past spatial fragmentation of this genus across the Mediterranean (Calvo et al., 2009).

Previous palaeosea-level studies applied a vertical uncertainty ranging between ±10 cm and ±20 cm to sublittoral *Dendropoma* spp. rims (Sivan et al., 2010 and references therein),

based on observations that *Dendropoma* spp must be continuously flushed by sea water (Safriel, 1975a,b; Laborel et al., 1994; Laborel and Laborel-Deguen, 1996; Antonioli et al., 1999; Silenzi et al., 2004). However, the precision of *Dendropoma* spp. *and V. triquetrus* aggregations as sea-level indicators has not been firmly established. Dean et al. (2019) determined the reef functional height in the Israeli coast, as the Mean Tidal level (MTL) with uncertainty between the mean high tidal level and the mean low tidal level. The Mediterranean is considered to be a low-tide region, yet, the mean high and low tide of Israel (Southeast Mediterranean) still vary by ~ 60 cm (Shirman, 2004; Rosen et al., 2016). Moreover, it is still not very clear how environmental factors, such as water temperature and wave energy, influence rim growth, but it seems that wave exposure might be important (Laborel, 1986).

Vermetus triquetrus is another reef building gastropod inhabiting the Mediterranean rocky shorelines alongside *Dendropoma* (Safriel, 1975a,b). However, very little is known about the vertical growth of *V. triquetrus* and its potential use as a sea-level indicator (Morhange et al., 2013).

The main aims of this paper are to study site-specific vertical reef development to improve the reliability of vermetid reefs as sea-level indicators and to better understand the spatial variability of their growth rates across the Mediterranean Sea. To achieve these goals, site-specific vertical growth and elevations have been studied based on radiocarbon dating and depth measurements from drilled cores, collected along a Mediterranean east-west transect, including Israel, Lebanon, Crete, Tunisia, Sicily and southern Spain (**Fig. 1**). Previously published elevations and radiocarbon ages on vermetid reefs from the Israeli coast (Sivan et al., 2010; Sisma-Ventura et al., 2014; Dean et al., 2019) and newly obtained data from the Galilee and the Carmel coasts, north Israel, have been used to evaluate the vertical uncertainties of

vermetid reefs as sea-level indicators. We further explore the importance of site-specific environmental factors, such as water temperature and nutrient content, on the reefs' vertical growth, using a detailed growth axis $\delta^{18}O$ analysis and site-specific meteorological data, sea-surface temperature (SST) and Chlorophyll a.

2. Methods

The paper combines previously published bio-construction sea-level markers (elevations and radiocarbon ages) from the Israeli coast (Sivan et al., 2010; Sisma-Ventura et al., 2014; Dean et al., 2019) and newly obtained data from Israel (**Table 1**), along with radiocarbon ages and depth measurements from drilled cores along a Mediterranean east-west transect, including Lebanon, Crete, Tunisia, Sicily and southern Spain (**Fig. 1** and **Supp. Table 1).**

2.1. Drilling, surveying and sampling

The rims formed by the Mediterranean *Dendropoma* complex of species were drilled vertically from the top of the ledges towards the rock substrate, using a pneumatic corer (with a 5 cm cup). The cores were cut with a diamond-head saw and sampled vertically from the top to the bottom for radiocarbon dating.

All previous Mediterranean studies mentioned above, including in Israel, measured the elevation of the reef surface manually, relative to the present sea level (using measuring rod) with corrections for local tide and atmospheric pressure at the time of measurements (Anzidei et al., 2011a and b). Newly obtained drillings from Israel in the Galilee and the Carmel (Dor) include measurements of the top surface of *Dendropoma* rims in each drilling point relative to the local Israel Land Survey Datum (ILSD) carried out with a RTK-DGPS system (RTK Proflex

500) (**Table 1**). In addition, surveys were carried out in four study sites spaced over 130 km along the coast, mapping the absolute elevations of reef ledges above the ILSD by first fixing benchmarks in each site using DGPS. A Trimble Spectra Precision Laser survey with a digital smart rod then measured the heights at multiple positions in three portions on the platforms: top of the *Dendropoma* rim (if it was present) at the seaward edge of the platform, behind the rim (a few cm at the rim's leeward side), and the platform center (1-3 m from the edge). The two portions behind the rim tend to be the *V. triquetrus* habitat (Rilov, 2016). This high-resolution spatial mapping provided the average elevations of the various portions of the reef relative to present tide levels.

Newly obtained radiocarbon ages were measured in eight reef structures along the Galilee coast, Northern Israel (**Table 1**), in sites which are characterized by multi-ledge morphologies. Samples were drilled in three sites and the surface of the bio-construction or the contact with the sandstone substrate were ^{14}C dated. Three new sea-level index points were obtained from two archeological coastal man-made structures containing bio-constructions of *V. triquetrus,* in the flushing channel of the fishpond of Achziv, and the flushing channels of Dor, Israel (**Fig. 1**). Samples were drilled in both sites and the bio-construction above the contact with the sandstone substrate was ^{14}C dated (**Fig. 2**). This newly obtained dataset is used in this study for re-assessing the vertical uncertainties of vermetid reefs.

2.2. Radiocarbon dating

Dendropoma spp. and *V. triquetrus* specimens were cut from the cores in slices of ~ 1 cm. They were separated by mechanical brushing and sonication. The organic matter was removed by washing cycles of 30% H_2O_2. Special care was taken to exclude any contamination, by

143 mechanically removing the red coralline algae cements, and by using the pristine inner shell

144 structure. Radiocarbon measurements were made at the ANSTO AMS Facility on homogenous

145 powders. The three samples overlying archaeological structures in Dor and in Achziv (Fig 1)

146 were dated in the Oxford Radiocarbon Accelerator Unit (United Kingdom). Radiocarbon

147 analyses of Mediterranean samples other than those from Israel were conducted in the

148 Radiocarbon Dating Laboratory, Australian National University, Australia. The radiocarbon

149 ages were converted into calendar years using the program Calib 7.0.1 (Stuiver and Reimer,

150 1993) and the Marine 13.14c calibration data set (Reimer et al., 2013). Basin-average reservoir

151 corrections ($\Delta R \pm R$) of 53$\pm$43 and 40$\pm$15 (^{14}C yr) were applied for raw ^{14}C measurements from

152 the east and west Mediterranean, respectively (Reimer and McCormac, 2002).

153

154 *2.3 Stable isotopes analysis*

155 In order to better understand the process of *Dendropoma* spp. and *V. triquetrus* skeleton

156 deposition, detailed $\delta^{18}O_{skeleton}$variability was measured along the growth axis of four living

157 *Dendropoma* specimens, collected from the Israeli coast (Achziv and Hazrot Yassaf). The

158 carbonate powders from the skeletons (200–250 µg, 0.4 mm drill) were dissolved in 100%

159 H$_3$PO$_4$ acid at 25°C for 24h and analyzed on a Gas Bench II connected to Finnigan MAT 252,

160 at the Weizmann Institute of Science. The results are reported relative to the VPDB standard

161 with long-term analytical precision of 0.08‰ ($\pm$1σ SD).

162 The average SST during vermetid skeleton deposition was calculated using the aragonite

163 temperature-dependent fractionation during bio-mineralization described by the Böhm et al.

164 (2000) equation:

165 $$(1) \ T°C = 20.4 - 4.43*(\delta^{18}O_{aragonite} - \delta^{18}O_{SW})$$

166 $\delta^{18}O_{aragonite}$ and $\delta^{18}O_{SW}$ are the isotope compositions of aragonite relative to VPDB and water

167 relative to the VSMOW standard, respectively. The Israeli coast annual average $\delta^{18}O_{SW}$ of

168 1.6±0.12‰ (Sisma-Ventura et al., 2014) was used for all calculations.

169 Site-specific mean annual SST and Chlorophyll a were obtained from the MEDATLAS

170 II (http://doga.ogs.trieste.it/medar/climatologies/), and were used to study the main factors,

171 influencing site-specific growth rate of *Dendropoma* spp.

172

3. Results

3.1. Elevations of reefs in Israel

175 Along most coasts in the Mediterranean, vermetid reefs appear as a single ledge at the edge of

176 the abrasion platform located close to MSL (**Fig. 3**). In Israel, the edge of the ledge surfaces

177 (where *Dendropoma* forms rims) was found to be slightly elevated relative to the Israel Land

178 Survey Datum (ILSD). Elevations gradually decrease southward (**Fig. 4**), averaging about

179 +0.51±0.07 m in the northernmost part of the Israeli coast, decreasing to about +0.3±0.09 m

180 and +0.13±0.05 m in the central and southern coasts, respectively, therefore, occupying the

181 upper intertidal zone, with a mean maximum height of +0.39±0.05 m (Rosen et al., 2013). The

182 areas just behind the rim and the central rock platform are a bit lower (**Fig. 4**) but the entire

183 abrasion platform is slightly elevated above MSL in the upper intertidal zone.

184 Along the northern Israeli coast, multi-ledge bio-constructions were observed in a few

185 specific sites: Akko, Hazrot Yasaf, Minet A-Ziv, Segavion Island (off Achziv) and Rosh

186 Hanikra (for locations see Fig. 1). An example of the multi ledge is seen in **Fig. 5** in Achziv,

187 where surface elevations of the reef tops vary between -0.27 m and +0.79±0.06 m (**Fig. 6** and

188 **Table 1**), thus occupying elevations above the maximum height of the mean tide. The ledge

189 surfaces yielded ^{14}C ages that are either modern and/or too recent to be dated with any

190 confidence considering the statistical uncertainty of the calibration and reservoir-corrected

191 range (**Table 1**). This indicates that the entire multi-ledge bio-construction has accumulated

192 approximately at the same time. Multiple ledge buildup was also observed in cores drilled from

193 the island of Segavion off Achziv in the north and along the coast of Akko (**Figs. 1** and **6**). This

194 complex reef structure was not observed south of Akko (**Fig. 1**).

195

196 *3.2. Vermetid reefs overlying archaeological structures*

197 In two archaeological sites, Dor, Carmel coast, and Achziv, Galilee coast (**Figs. 1** and **2**), bio-

198 constructions overlying historical man-made structures related to past sea level were drilled.

199 The bio-constructions infilling the Achziv channel date to the end of the 15th century - the

200 beginning of the 16th century, (**Fig. 2** and **Table 1**). The two ages of Achziv are almost identical,

201 which strengthens their reliability. At Dor, the shells of *V. triquetrus* are dated to around the

202 mid-late 18th century. These new ages also provide new RSL index points, and confirm that the

203 structures on which the organism grew were cut and formed at an indeterminate time before the

204 dates shown in **Table 1**.

205

206 *3.3. The vertical profiles of vermetid rims*

207 Down core profiles of the rims are typically composed of *Dendropoma* shells, but can also

208 include shells of *V. triquetrus* up to 10 cm thick as was observed along the northern Israeli coast

209 (**Fig. 7**). Here *V. triquetrus* is the main gastropod covering the back reef rocky platforms.

However, *V. triquetrus* can also be found alongside and without *Dendropoma* as part of the rim's structure (**Figures 6** and **7**).

3.4. Vertical growth rates of Dendropoma *from various sites along the Mediterranean*

The vertical profiles obtained from *Dendropoma* spp. shells, cemented by a thin layer of red coralline algae, show a typical structure. All core tops were either alive or dated modern by ^{14}C analysis, confirming reef growth up to present, or die-off in the last few decades. The $\delta^{13}C$ average composition of 0.3±1.3‰ in Table 1 is a typical value for modern *Dendropoma* shells (Sisma-Ventura et al., 2014). When comparing the data around the Mediterranean sites, the oldest radiocarbon ages (~2800 cal. yr. BP) were obtained from the *D. cristatum* cores drilled in NW Sicily, while those from Spain and Israel are ~1400 cal. yr. BP and ~1000 cal. yr. BP, respectively (**Fig. 8**).

Different rates of vertical growth were observed for *Dendropoma* spp. rims in various Mediterranean sites. The results in **Fig. 8** show mostly continuous vertical growth over several centuries for the cores drilled along the northern Israeli coast and in Crete, and over several millennia for NW Sicily, Spain and Tunisia. Gaps in rims growth are visible in the *D. anguliferum* cores from the Israeli coast, between 800 and 600 cal. yr. BP, and along the Sicilian coast around 1500 cal. yr. BP. Available growth data are not evenly distributed across the sites. The two sites that contain a relatively high amount of data are Israel and NW Sicily. The highest rates were measured along the Israeli coast (average rate of 1.04±0.15 mm yr^{-1}) compared to an average rate of 0.18±0.03 mm yr^{-1} for NW Sicily. In the western Mediterranean, the Spanish coast drillings yielded average vertical growth rates of 0.13±0.09 mm yr^{-1} (**Table 2**). A single core from Crete provides a continuous vertical growth of 1.0 mm yr^{-1} (uncertainty was not

233   calculated since there is only one core). Growth rates for samples collected along the coast of

234   Lebanon and Tunisia could not be calculated due to the limited number of available ^{14}C ages.

235

236   *3.5. Oxygen isotope analyses*

237   Samples collected along the vermetid growth axis of four living specimens in different sites (all

238   from the northern Israeli coast) yielded $\delta^{18}O$ ranging from -0.4 to 1.9‰ (**Fig. 9**). The growth

239   axis $\delta^{18}O$ in vermetid DP-1 (from Achziv) suggests a cyclic deposition covering two cycles

240   while those of DP-3 (from Achziv) and DP-4 (from Hazrot Yassaf) indicate a lifespan of only

241   one year. The growth axis $\delta^{18}O$ range is translated to depositional temperatures between 19 and

242   30°C, where 73% of calcification occurs above the mean annual SST of 23.5°C. An average

243   SST for deposition of 25.3±3.0°C was calculated among the four specimens, ranging between

244   22.5±2.7°C in sample DP-4 (Hazrot Yassaf) and 27.5±2.5°C in DP-2 (Achziv), indicating a

245   preferential warm water skeleton deposition. The maximum SST for deposition was close to

246   30°C, while the minimum was around 19°C.

247

248   **4. Discussion**

249   *4.1. Vermetid reefs in Israel as sea-level indicators*

250   *Dendropoma* spp. reefs have been used as a sea-level marker both in the western (Antonioni et

251   al., 1999; Silenzi et al., 2004) and eastern basins of the Mediterranean (Dean et al., 2019). These

252   studies used vertical uncertainties of ±0.1 to ±0.2 m and showed decimeter-scale sea-level

253   changes during the last millennium. Based on his observations in Israel, Safriel (1975a,b)

254   suggested that the rims of the Carmel coast are low intertidal bioconstructions, with living tops

255   located very close to the mean sea level.

Unlike previous Mediterranean studies that measured elevations manually relative to sea level with corrections for tide and atmospheric pressure at the time of measurements (Anzidei et al., 2011a and b), our new core elevations from Israel (including the archaeological sites) are based on DGPS measurements relative to the ILSD. When using previous data, we have to bear in mind that a sea-level rise of ~6 cm relative to the ILSD has been calculated by Shirman (2004) for the years 1958 to 2001. Sea level has continued to rise since then and is now estimated to be ~12 cm above the ILSD (Rosen et al., 2013). In addition, we provide new elevation data from four sites along the coast of Israel based on Laser measurements, again, relative to the ILSD.

Our DGPS data (relative to the ILSD) show that the abrasion platforms of the Carmel coast (Shikmona and Dor) are located relatively close to MSL, but the rim tops at the seaward edge of the platform are always slightly elevated above the rest of the platform surface (platform center). Vermetid reef platforms vary considerably in shape and size along the Israeli coast (Rilov et al 2004), but there seems to be a pattern of a general decrease in elevation southward from 0.51±0.07 m in the Galilee to 0.35±0.09 m in the Carmel coast and to only 0.13±0.05 m at Palmachim (**Fig. 4**). In Palmachim there is no visible *D. anguliferum* rim as also mentioned by Tzur and Safriel, (1978). It seems that terrace shaped multi-ledge bioconstructions are found only in the Galilee coast, where the rims may develop above and slightly below the intertidal zone (**Figs. 5** and **6**). On the Carmel coast (Shikmona and Dor/Habonim) and in places around Achziv, the rims are found almost at MSL.

Dean et al. (2019) have used down-core ^{14}C ages of *D. anguliferum* from the Israeli coast to reconstruct RSL changes during the last millennium. Previously, most of the data had been obtained from cores drilled along the Carmel coast, where the top of the cores containing living

279   *Dendropoma* was considered to represent MSL. In the current study, the Dor core top has been

280   measured by DGPS yielding an elevation of +0.18 m (Table 1). Taking into account the present

281   +0.12 m estimated sea-level elevation relative to the ILSD, we can confirm that the top core is

282   about +0.06 ± 0.05 m relative to present MSL. It also confirms the reliability of previous

283   elevations from the Carmel coast: Dor, Habonim, Atlit and Shikmona (Dean et al., 2019).

284   However, sea-level data that were obtained from places with multi-ledge morphologies like

285   Achziv (**Fig. 5**) can carry higher vertical uncertainties. In some places the modern tops of the

286   reefs vary between -0.30 m and +0.80 m relative to the ILSD (**Fig. 6**) and therefore, are not

287   ideal sea-level indicators.

288

289   ***4.2. Archaeological implications as a test case from Israel***

290   The new ages obtained in the current study from *V. triquetrus* overlying man-made structures

291   produce new sea-level index points, but they do not provide information on when these

292   structures were built or for how long they were used. For example, the ~400 cal. yr. BP dates

293   from Achziv (**Table 1** and **Fig. 2**) postdate the Roman ages inferred from archaeological

294   excavations at the site (Ratzlaff et al., 2012). Some additional useful information on the pools

295   can be obtained by dating the infilling bio-constructions. The settlement of *V. triquetrus* in the

296   flushing channel of Achziv during the end of the 15th century or the beginning of the 16th century

297   corresponds with a period of rising sea level (Dean et al., 2019). The preservation of *V.*

298   *triquetrus* rims inside the channel can be explained by relatively moderate flow in the channel

299   that protected it from sea abrasion. A lack of *V. triquetrus* from the Crusader Period indicates

300   no continuing flushing of the channel during periods of low sea levels (Toker et al., 2012; Dean

301   et al., 2019). According to the RSL curve of Israel, the last time the Achziv pool was functioning

302   is therefore during periods of relatively high sea level, i.e. the Roman-Byzantine period.

303

304   *4.3. Vertical growth as a function of temperature and wave energy*

305   *Dendropoma* rims are found in the warm waters of the southeastern and southwestern

306   Mediterranean. There are a few observations of developing rims in Corsica (Laborel, 1986) and

307   some structures in north-western Sardinia (Chemello & Silenzi, 2011). This spatial distribution

308   was described by Antonioli et al. (1999) suggesting that SST is a key factor regulating the rim

309   growth of *D. petraeum* across the Mediterranean. Dated cores show higher vertical growth rates

310   in the eastern Mediterranean (Crete, although based on a single core, and Israel) compared to

311   the western basin (**Fig. 8**), suggesting the importance of the water temperature as a driving

312   factor. Site-specific growth rates as a function of mean annual SST and chlorophyll-a are

313   presented   in   **Figure   10**   (data   from   MEDATLAS   II;

314   http://doga.ogs.trieste.it/medar/climatologies/), showing opposite trends: growth rate is higher

315   in the east where temperatures are high and nutrient availability is low. This implies that

316   temperature (Mediterranean gradient shown in **Figure 11**) rather than food availability is the

317   likely cause for the differences in vertical growth of *Dendropoma* rims between the eastern and

318   western Mediterranean.

319   This conclusion can also be inferred from the $\delta^{18}O$ record in the vermetid tubes, measured

320   along the growth axis of shells from the Israeli coast (**Fig. 9**). The calculated depositional

321   temperatures show that most calcification occurs in summer (between 25-30ºC), while below

322   about 19 ºC calcification is strongly reduced. The lower temperature ranges of the western

323   basin, varying between 14 and 26ºC (**Figure 11**), support lower growth rate and possibly a

shorter seasonal growth period of vermetids, compared to specimens from the eastern basin (temperature range of 17-31 ºC), although this was not measured for single specimens from the western basin. Different intrinsic growth rates might also contribute to the observed difference in growth between the eastern and western Mediterranean *Dendropoma* species. The higher growth rates of *D. anguliferum* along the Israeli coast therefore offers higher resolution (5-6 years) records of paleo-oceanographic and RSL changes (Sisma-Ventura et al., 2009; 2014; Bialik and Sisma-Ventura, 2016; Dean et al., 2019).

The $\delta^{18}O$ record measured along the growth axis also indicates maximum calcification temperatures around 30 ºC, supporting the hypothesis of Rilov (2016) that the recent rapid warming of the southeastern Mediterranean surface waters by ~1 ºC per decade over the last 30 years (Ozer et al., 2016) may have contributed to the collapse and near extinction of *Dendropoma* populations in the southeastern Mediterranean.

Our results show the development of multi-ledge bio-constructions at specific sites along the northern Israeli coast with a vertical thickness of more than 1 m (**Fig. 5** and **6**). Radiocarbon ages indicate that the entire multi-ledge bio-constructions formed over a very short time, maybe because they are subjected to relatively high wave activity that continuously flushed the reefs. Indeed, the nearshore waters of the northern Israeli Mediterranean coast are subjected to a high degree of wave exposure. For example, based on 5510 measurements in Haifa, Rilov et al. (2005) calculated that 94% had a maximum wave height of >0.5 m, and 57% had a wave height of >1 m. In northern Israel wave conditions can therefore promote reef development above the intertidal zone. These findings along the northern Israeli coast indicate that the *D. anguliferum* reefs are a site-specific sea-level indicator, displaying variable indicative ranges. This confirms

346 earlier observations of vermetid reefs by Laborel (1986) and Rovere et al. (2015) who also

347 suggested that their vertical ranges depend on wave exposure.

348   The complex inner structure of the rims along the northern Israeli coast, at times

349 containing juxtapositions of *D. anguliferum* and *V. triquetrus* (**Fig. 7**), is intriguing and may

350 be partly related to high abrasion rates, again due to the high degree of wave exposure, which

351 breaks the edge of the rim. Consequently, the central part of the platform, which is inhabited by

352 *V. triquetrus* only, can become the edge fronting the sea. However, other factors such as

353 storminess and ecological impacts cannot be ruled out (Dulin et al., 2020).

354

355 **5. Conclusions**

356 1. Biological markers like the *Dendropoma petraeum* complex of species and *Vermetus*

357 *triquetrus* are considered reliable sea-level indicators. Previous sea-level estimates based on

358 these markers included relatively small vertical uncertainties of ±0.1 m to ±0.2 m. However,

359 our observations based on Differential Global Positioning System (DGPS) and laser

360 measurements relative to the ILSD, reveal that these markers are more complicated as they can

361 develop multi-ledge bio-constructions where uncertainty is larger (up to about 1 m), especially

362 in northern Israel where the platform is 40-50 cm above the ILSD. Therefore, whenever

363 vermetid reefs are used to reconstruct past RSL change, the vertical uncertainty needs to be

364 evaluated for each site based on the local structure and environmental conditions.

365 2. The rates of growth of the reefs vary by 10-fold between basins and are probably

366 environment-dependent. Water temperature is suggested to be the main factor affecting their

367 growth, with our test cases showing the fastest growth rate in summer (25-30°) and reduced

368 calcification below ~19°. Different growth rates can affect the age/depth model accuracy since

369 long cores produce more samples and different length core can represent very different dating.

370 3. The *Dendropoma petraeum* complex of species can be used as a sea-level indicator based on

371 the understanding that their upper part represents the upper subtidal zone and therefore can be

372 treated as a "biological sea-level" marker. The elevations of the upper living part should be

373 measured relative to the local datum (ILSD). In almost all previously published datasets, no

374 measurements relative to the local Datum were carried out. Surveying relative to the local datum

375 should reduce the uncertainty when comparing between remote datasets. We therefore

376 recommend measuring top elevations relative to local datum rather than to arbitrary tide levels.

377

393

394

References

Antonioli, F., Chemello, R., Improta, S., Riggio, S. 1999. Dendropoma lower intertidal reef formations and their palaeoclimatological significance, NW Sicily. Marine Geology, 16, 155–170.

Antonioli, F., Lo Presti, V., Rovere, A., Ferranti, L., Anzidei, M., Furlani, S., Mastronuzzi, G., Orru, E.P., Scicchitano, G., Gianmaria, S, Spampinato, R.C. Pagliarulo, R., Giacomo, D., de Sabata, E., Sansò, P., Vacchi, M., Vecchio, A. 2015. Tidal notches in Mediterranean Sea: a comprehensive analysis, Quaternary Science Reviews, 119(1), 66–84.

Antonioli, F., Ferranti, L., Stocchi, P., Deiana, G., Lo Presti, V., Furlani, S., Marino, C. 2018. Morphometry and elevation of the last interglacial tidal notches in tectonically stable coasts of the Mediterranean Sea, Earth-Science Reviews, 185, 600–623.

Amitai, Y., Yam, R., Montagna, P., Devotic, S., Matthias L´opez Correa L.M., Shemesh., A. 2020. Spatial and temporal variability in Mediterranean climate over the last millennium from vermetid isotope records and CMIP5/PMIP3 models, Global and Planetary Change, 189, 103159.

Anzidei, M., Antonioli, F., Benini, A., Lambeck, K., Sivan, D., Serpelloni, E., Stocchi, P., 2011a. Sea level change and vertical land movements since the last two millennia along the coasts of southwestern Turkey and Israel. Quaternary International, 232, 13–20.

Anzidei, M., Antonioli, F., Lambeck, K., Benini, A., Soussi, M., Lakhdar, R., 2011b. New insights on the relative sea level change during Holocene along the coasts of Tunisia and western Libya from archaeological and geomorphological markers. Quaternary International, 232, 5–12

Bialik, M.O., Sisma-Ventura, G. 2016. Proxy-based reconstruction of surface water acidification and carbonate saturation of the Levant Sea during the Antropocene, Antropocene, 16, 42–53.

Bohm, F., Joachimski, M.M., Dullo, W.C., Eisenhauer, A., Lehnert, H., Reitner, J., Worheide, G.2000. Oxygen isotope fractionation in marine aragonite of coralline sponges, Geochim. Cosmochim. Acta, 64(10), 1695–1703.

Calvo, M., Templado, J., Oliverio, M., Machordom, A. 2009. Hidden Mediterranean biodiversity: molecular evidence for a cryptic species complex within the reef building vermetid gastropod *Dendropoma petraeum* (Mollusca: Caenogastropoda). Biological Journal of the Linnean Society, 96, 898–912.

Chemello, R., Silenzi, S. 2011. Vermetid reefs in the Mediterranean Sea as archives of sea-level and surface temperature changes. Chemistry and Ecology, 27(2), 121–127.

Dean, S., Horton, B.P., Evelpidou, N., Cahill, N., Spada, G., Sivan, D. 2019. Can we detect centennial sea-level variations over the last three thousand years in Israeli archaeological records? Quaternary Science Reviews, 210, 125–135.

Dulin, T., Avnaim-Katav, S., Bialik, M.O., Sisma-Ventura, G., Angel D. 2020. Rhodolith beds along the southeastern Mediterranean inner shelf: Implications for past depositional environments, Journal of Marine Systems, 201, 103241.

Faivre, S., Bakran-Petricioli, T., Horvatinčić, N., Sironić, A. 2013. Distinct phases of relative sea level changes in the central Adriatic during the last 1500 years – influence of climatic variations?, Palaeogeography, Palaeoclimatology, Palaeoecology, 369, 163–174.

Faivre, S., Bakran-Petricioli, T., Barešić, J., Horvatić, D., Macario, K. 2019. Relative sea level change and climate change in the Northeastern Adriatic during last 1.5 ka (Istria, Croatia), Quaternary Science Reviews, 222, 105909.

Ferranti, L., Antonioli, F., Amorosi, A., Dai Pra, G., Mastronuzzi, G., Mauz, B., Monaco, C., Orrú, P., Pappalardo, M., Radtke, U., Renda, P., Romano, P., Sanso, P., Verrubbi, V. 2006. Elevation of the

439   Last Interglacial highstand in Sicily (Italy): a benchmark of coastal tectonics. Quaternary International,
440   145–146, 30–54.
441   Laborel, J. 1986. Vermetid Gastropods as Sea-level Indicators. In: van de Plassche, O. (Ed.), Sea-Level
442   Research: A Manual for the Collection and Evaluation of Data. Geo Books, Norwich, Amsterdam, pp.
443   281–310.
444   Laborel, J., Morhange, C., Lafont, R., Le Campion, J., Laborel-Deguen, F., Sartoretto, S. 1994. Biological
445   evidence of sea-level rise during the last 4500 years on the rocky coasts of continental southwestern
446   France and Corsica. Marine Geology, 120, 203–223.
447   Laborel, J., Laborel-Deguen, F. 1996. Biological indicators of Holocene sea-level and climatic variations
448   on rocky coasts of tropical and subtropical regions. Quaternary International, 31, 53–60.
449   Lambeck, K., Purcell, A. 2005. Sea-level change in the Mediterranean Sea since the LGM: model
450   predictions for tectonically stable areas. Quaternary Science Reviews, 24, 1969–1988.
451   Lambeck, K., Antonioli, F., Purcell, A., Silenzi, S. 2004. Sea-level change along the Italian coast for the
452   past 10,000 yr. Quaternary Science Reviews, 23, 1567–1598.
453   Milne, G.A., Mitrovica, J.X. 2008. Searching for eustasy in deglacial sea-level histories. Quaternary
454   Science Reviews, 27, 2292–2302.
455   Morhange, C., Pirazzoli, P.A., Marriner, N., Montaggioni, L.F., Nammour, T. 2006. Late Holocene relative
456   sea-level changes in Lebanon, Eastern Mediterranean. Marine Geology, 230, 99–114.
457   Morhange, C., Marriner, N., Excoffon, P., Bonnet, S., Flaux, C., Zibrowius, H., Goiran, J., Amouri, M.E.
458   2013. Relative sea-level changes during Roman times in the northwest Mediterranean: the 1st century
459   AD fish tank of Forum Julii, Fréjus, France. Geoarchaeology, 28(4), 363–372.
460   Morhange C., Marriner N. 2015. Archeological and biological relative sea-level indicators, In: Shennan I.,
461   Long A. J., Horton B. P. (eds), "Handbook of Sea Level Research" Wiley, Chap. 9, pp. 146–156
462   Ozer, T., Gertman, I., Kress, N., Silverman J., Herut, B. 2016. Interannual thermohaline (1979-2014) and
463   nutrient (2002-2014) dynamics in the Levantine surface and intermediate water masses, SE
464   Mediterranean Sea. Global Planetary Change, 151: 60–67.
465   Pirazzoli, P.A., Laborel, J., Saliège, J.F., Erol, O., Kayan, I., Person, A. 1991. Holocene raised shorelines
466   on the Hatay coasts (Turkey: paleoecological and tectonic implications). Marine Geology. 96, 295–
467   311.
468   Pirazzoli, P.A., Stiros, S.C., Arnold, M., Laborel, J., Laborel-Deguen, F., Papageorgiou, S. 1994. Episodic
469   uplift deduced from Holocene shorelines in the Perachora Peninsula, Corinth area, Greece.
470   Tectonophysics, 229, 201–209.
471   Ratzlaff, A., Yassur-Landau, A., Davies, G. 2012. Excavation at Tel Achziv 2012 Season (Archaeological
472   Report (Preliminary) No. G-10/2012). University of Haifa/Israel Antiquities Authority, Haifa.
473   Reimer P.J., McCormac, F.G. 2002. Marine radiocarbon reservoir corrections for the Mediterranean and
474   Aegean Seas. Radiocarbon, 44, 159–166.
475   Reimer, P.J., Bard, E., Bayliss, A., Beck, J.W., Blackwell, P.G., Bronk Ramsey, C., Buck, C.E., Cheng, H.,
476   Edwards, R.L., Friedrich, M., Grootes, P.M., Guilderson, T.P., Haflidason, H., Hajdas, I., Hatte, C.,
477   Heaton, T.J., Hoffmann, D.L., Hogg, A.G., Hughen, K.A., Kaiser, K.F., Kromer, B., Manning, S.W.,
478   Niu, M., Reimer, R.W., Richards, D.A., Scott, E.M., Southon, J.R., Staff, R.A., Turney, C.S.M., van
479   der Plicht, J. 2013. IntCal13 and Marine13 radiocarbon age calibration curves 0-50,000 years cal BP.
480   Radiocarbon, 55(4), 1869–1887.
481   Rilov, G., Benayahu, Y., Gasith, A. 2004. Prolonged lag in population outbreak of an invasive mussel: a
482   shifting-habitat model. Biological Invasions, 6(3), 347–364.

483 Rilov, G., Gasith, A., Benayahu, Y. 2005. Effect of disturbance on foraging: whelk activity
484   on wave-exposed rocky shores with minimal tidal range. Marine Biology, 147, 421–428.
485 Rilov, G. 2016. Multi-species collapses at the warm edge of a warming sea. Science Reports, 6, 36897
486 Rosen, S. D., Raskin, L., Galanti, B. 2013. Long-term characteristics of sea level, wave, wind and current
487   at central Mediterranean coast of Israel from 20 years of data at GLOSS station 80 - Hadera. Paper
488   presented at the 40th CIESM Congress, Marseille.
489 Rovere, A., Antonioli, F., Bianchi, C.N. 2015. Fixed Biological Indicators. In: Shennan, I., Long, A.J.,
490   Horton, B.P. (Eds.), Handbook of Sea Level Research. Wiley, pp. 268–280.
491 Safriel, U.N. 1975a. Vermetid Gastropods and Intertidal Reefs in Israel and Bermuda. Science, 186
492   (4169), 1113–1115.
493 Safriel, U.N. 1975b. The role of vermetid gastropods in the formation of Mediterranean and Atlantic reefs.
494   Oecologia, 20, 85–101.
495 Shirman, B., 2004. East Mediterraneasn sea level changes over the period 1958-2001. Israel Journal of
496   Earth Sciences, 53, 1–12
497 Silenzi, S., Antonioli, F., Chemello, R. 2004. A new marker for sea surface temperature trend during the
498   last centuries in temperate areas: Vermetid reef. *Global and Planetary Change,* 40, 105–114.
499 Sisma-Ventura, G., Guzner, B., Yam, R., Fine, M., Shemesh, A. 2009. The reef builder gastropod
500   *Dendropoma petraeum* - A proxy of short and long term climatic events in the Eastern Mediterranean.
501   Geochimica et Cosmochimica Acta, 73, 4376–4383.
502 Sisma-Ventura, G Yam, R., Shemesh, A. 2014. Recent unprecedented warming and oligotrophy of the
503   eastern Mediterranean Sea within the last millennium, Geophysical Research Letters,
504   DOI: 10.1002/2014GL060393.
505 Sisma-Ventura, G., Sivan, D., Steinberg, G., Bialik, O.M., Greenbaum, N. 2017. Last interglacial sea level
506   high-stands, deduced from abrasive notches, exposed at the Galilee coast, Israel. Palaeogeography,
507   Palaeoclimatology, Palaeoecology, 470, 1–10.
508 Sivan, D., Wdowinski, S., Lambeck, K., Galili, E., Raban, A. 2001. Holocene sea-level changes along the
509   Mediterranean coast of Israel, based on archaeological observations and numerical model.
510   Palaeogeography, Palaeoclimatology, Palaeoecology, 167, 101–117.
511 Sivan, D., Lambeck, K., Toueg, R., Raban, A., Porath, Y., Shirman, B. 2004. Ancient coastal wells of
512   Caesarea Maritima, Israel, an indicator for sea level changes during the last 2000 years. Earth and
513   Planetary Science Letters, 222, 315–330.
514 Sivan, D., Schattner, U., Morhange, C., Boaretto, E. 2010. What can a sessile mollusk tell about the
515   Neotectonics of EasternMediterranean? Earth and Planetary Science Letters, 296(3–4), 451–458.
516 Sivan, D., Sisma-Ventura, G., Greenbaum, N., Bialik, O.M., Williams, F.H., Tamisiea, M.E., Rohling, E.J.,
517   Frumkin, A., Avnaim-Katav, S., Shtienberg, G., Stein, M. 2016. East Mediterranean Sea levels through
518   the last interglacial from a coastal-marine sequence in northern Israel. Quaternary Science Reviews,
519   145, 204–225.
520 Stuiver, M., Reimer, P.J. 1993. Extended ^{14}C data base and revised CALIB 3.0 ^{14}C age calibration program.
521   Radiocarbon, 35, 215–230.
522 Templado, J., Richter, A., Calvo, M. 2016. Reef building Mediterranean vermetid gastropods: disentangling
523   the Dendropoma petraeum species complex. Mediterranean Marine Science, 17, 13–31.
524 Toker, E., Sivan, D., Stern, E., Shirman, B., Tsimplis, M., Spada, G. 2012. Evidence for centennial scale
525   sea level variability during the Medieval Climate Optimum (Crusader Period) in Israel, eastern
526   Mediterranean. Earth and Planetary Science Letters, 315–316, 51–6.

527   Tzur, Y., Safriel, U.N. 1978. Vermetid platforms as indicators of coastal movement. Israel Journal of
528   Earth Sciences, 124–127.

529

530   **Figures**
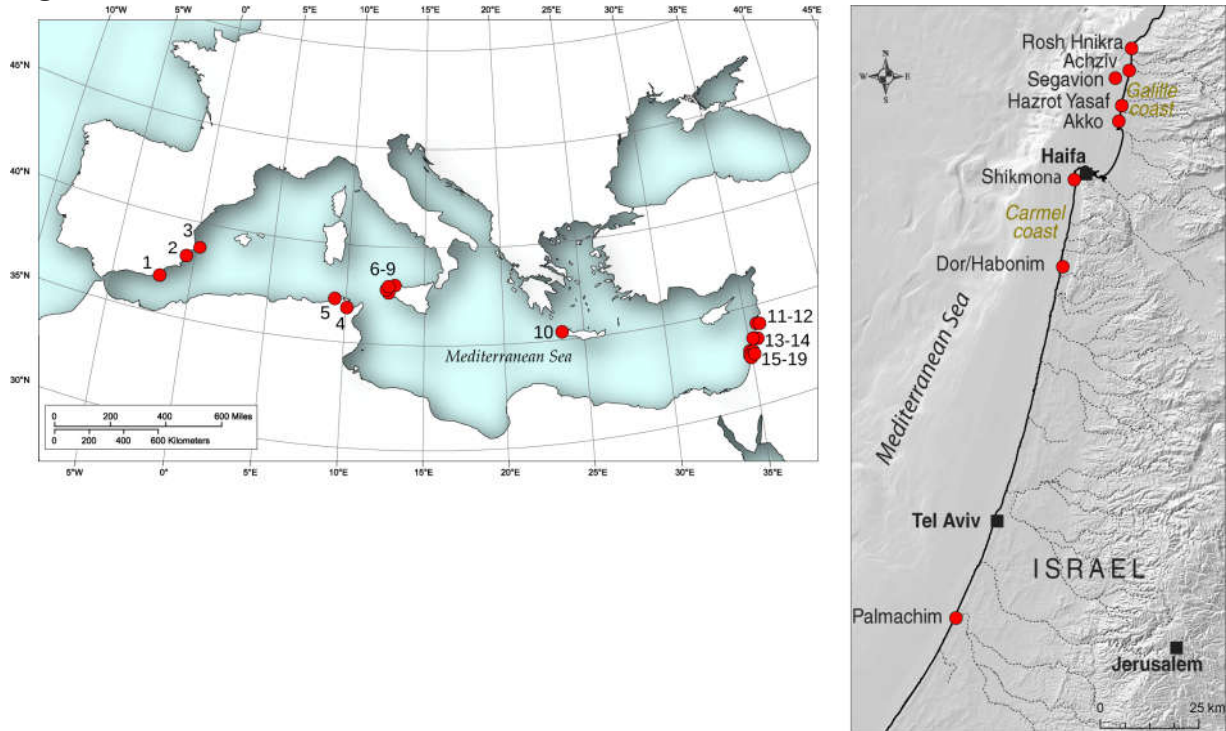
531

532   **Fig. 1.** Study-site maps: the numbers describe the drilling sites of *Dendropoma petraeum* complex
533   (a) along a Mediterranean West-East transect and (b) along the Israeli coast, including site-specific
534   DGPS and laser mapping.
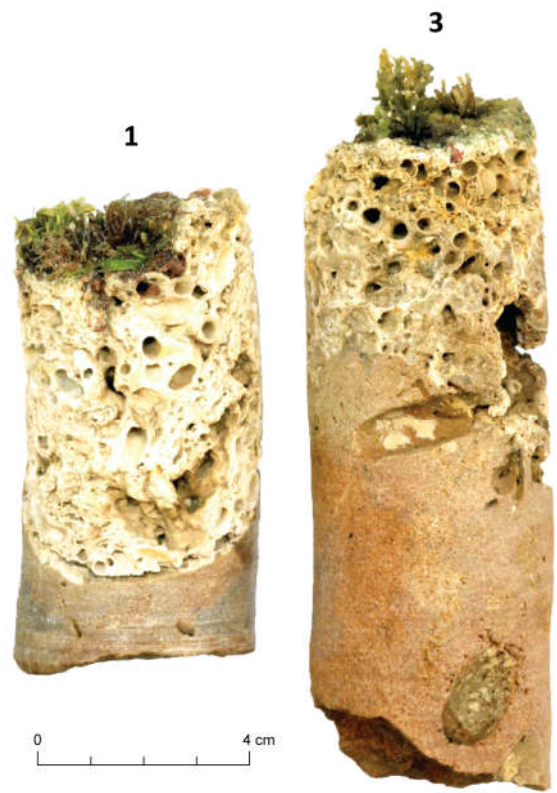
Fig. 2. Drilling positions of bio-constructions and retrieved cores of *V. triquetrus* infilling the flushing channel of the fishpond in Achziv.

Fig. 3. Photos of vermetid reefs and drill holes showing the different morphologies of *Dendropoma* spp. rims at our study sites: (a-b) are from Spain (c-d) are from NW Sicily, (e-f) are from Create and (g-h) are from Israel.
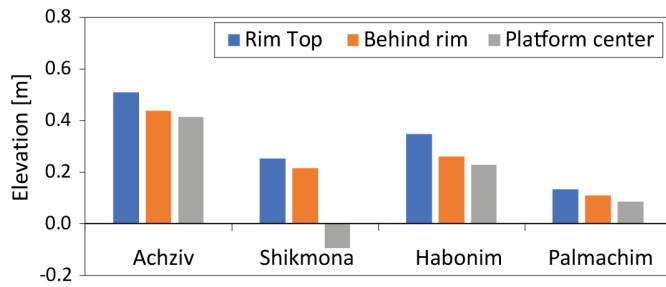
Fig. 4. Site-specific DGPS and laser mean elevations of four reef sites along the Israeli coast: Achziv, Shikmona, Habonim-Dor, Palmachim, and the three studied vertical zones: top of the rim, bottom of the rim on the leeward side (behind rim), and the platform center. Measurements relative to the Israel Land Survey Datum (ILSD).

Fig. 5. The Achziv coast multi-ledge bio-constructions during low tide showing three exposed ledges. There are two more submerged ledges. The entire structure occupying a vertical thickness of more than 1 m.
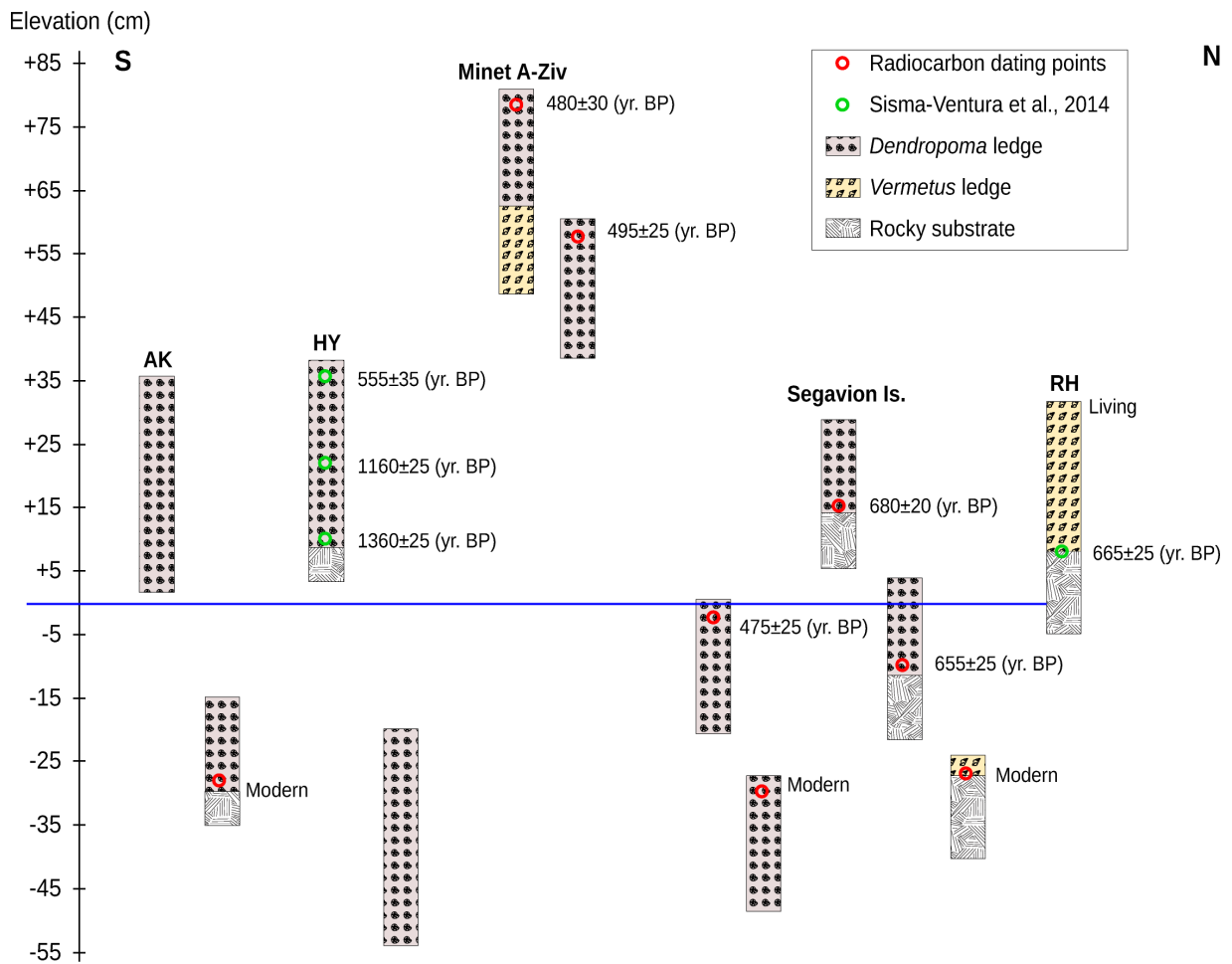
Fig. 6. An illustration showing the relative vertical and temporal (^{14}C age) locations of the multi-ledge bio-constructions along the Galilee coast, north Israel; Ak is Akko, HY is Hazrot Yasaf, Rh is Rosh Hanikra (See **Figure 1**). The ledges also present the interplay between the two reef building gastropods *D. anguliferum* and *V. triquetrus*.
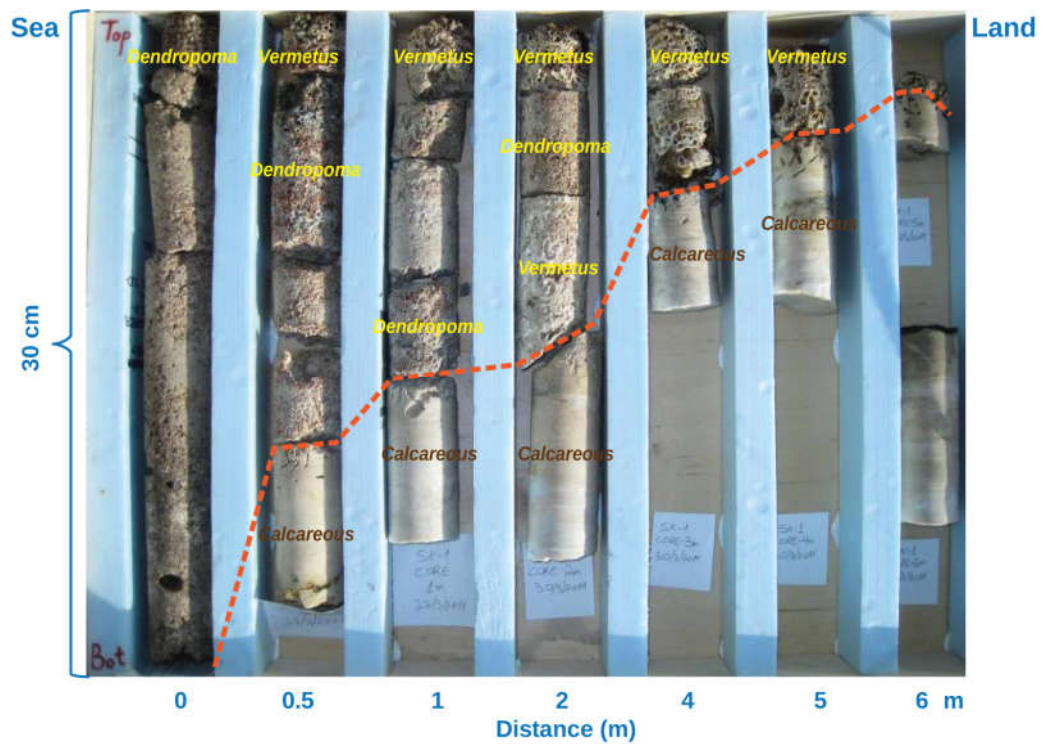
Fig. 7. Horizontal and vertical alternations of *V. triquetrus* and *D. anguliferum,* Shikmona, Israel
(**Fig. 1**), in a series of cores perpendicular to the shore presenting the transition from *Dendropoma*
to *Vermetus* and shallowing of the biogenic crust from the edge to the back of the reef.
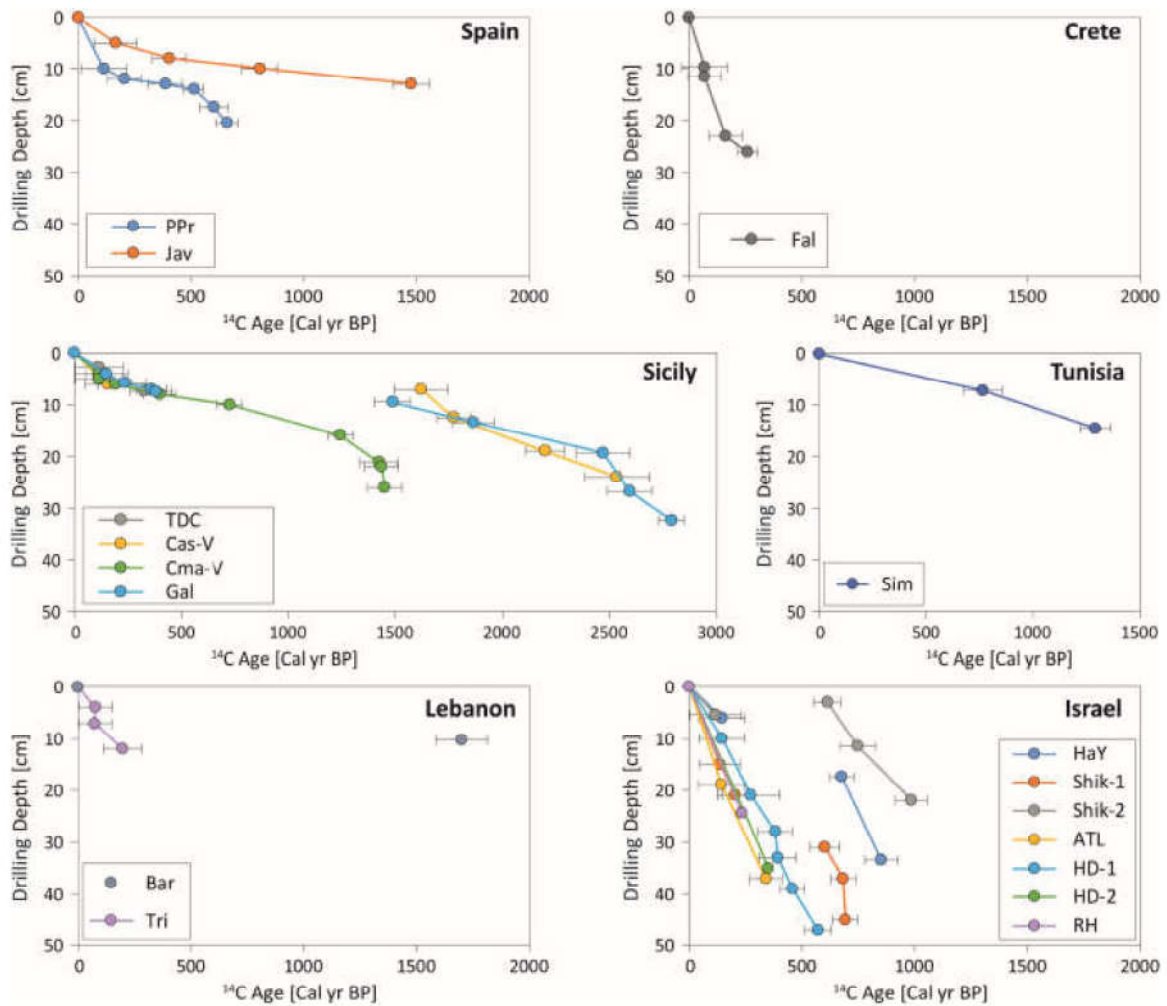
561
Fig. 8. Vertical growth rates (drilling depth vs. ^{14}C age) of vermetid reefs along a Mediterranean west-east transect. All data, except from Israel (Sisma-Ventura, 2014), are newly obtained and presented for the first time in the current paper. The vermetids of the western basin show older ages, but relatively low rates, compared to the much younger ages and higher growth rates in the eastern basin.
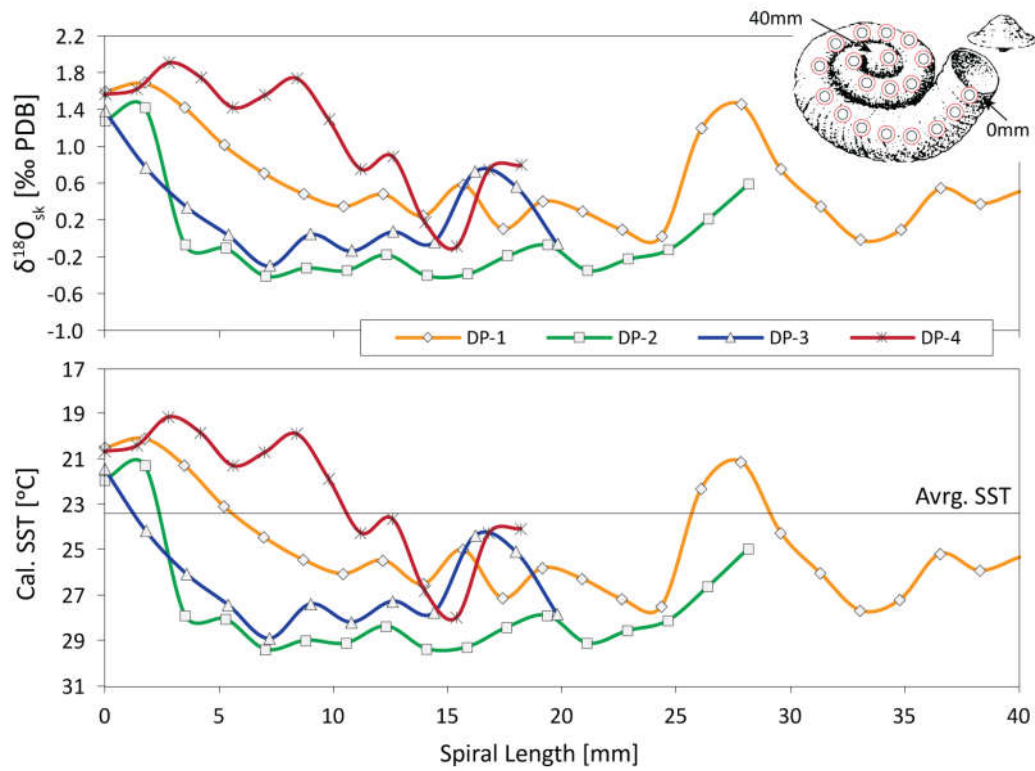
Fig. 9. Growth axis δ¹⁸O analysis and calculated SST of deposition in four *Dendropoma* samples from the Israeli coast; samples DP-1, 2 and 3 are from Achziv and DP-4 from Hazrot Yassaf. The data presented show preferential skeleton deposition in warm water.
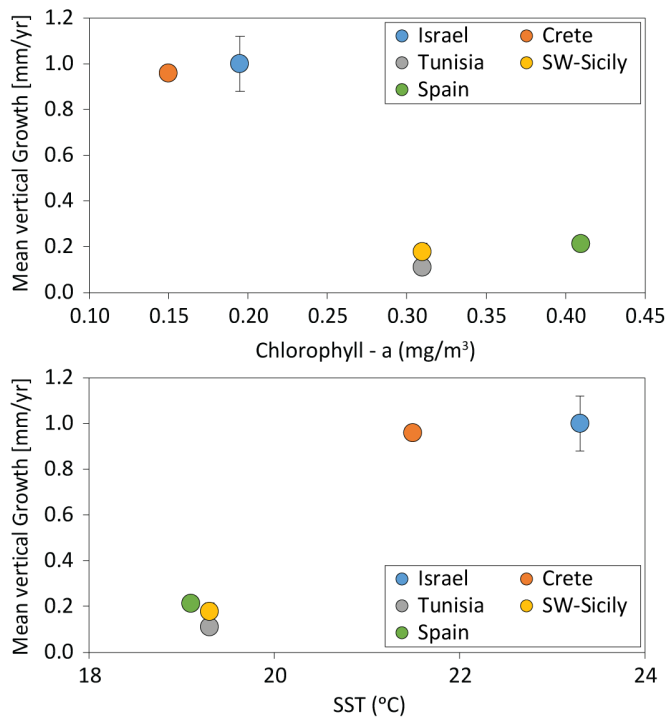
Fig. 10. Site-specific growth rates as a function of mean annual sea surface temperature and chlorophyll-a (data from MEDATLAS) showing that temperature is likely the key factor regulating the vertical growth of the different *Dendropoma* species in the Mediterranean.
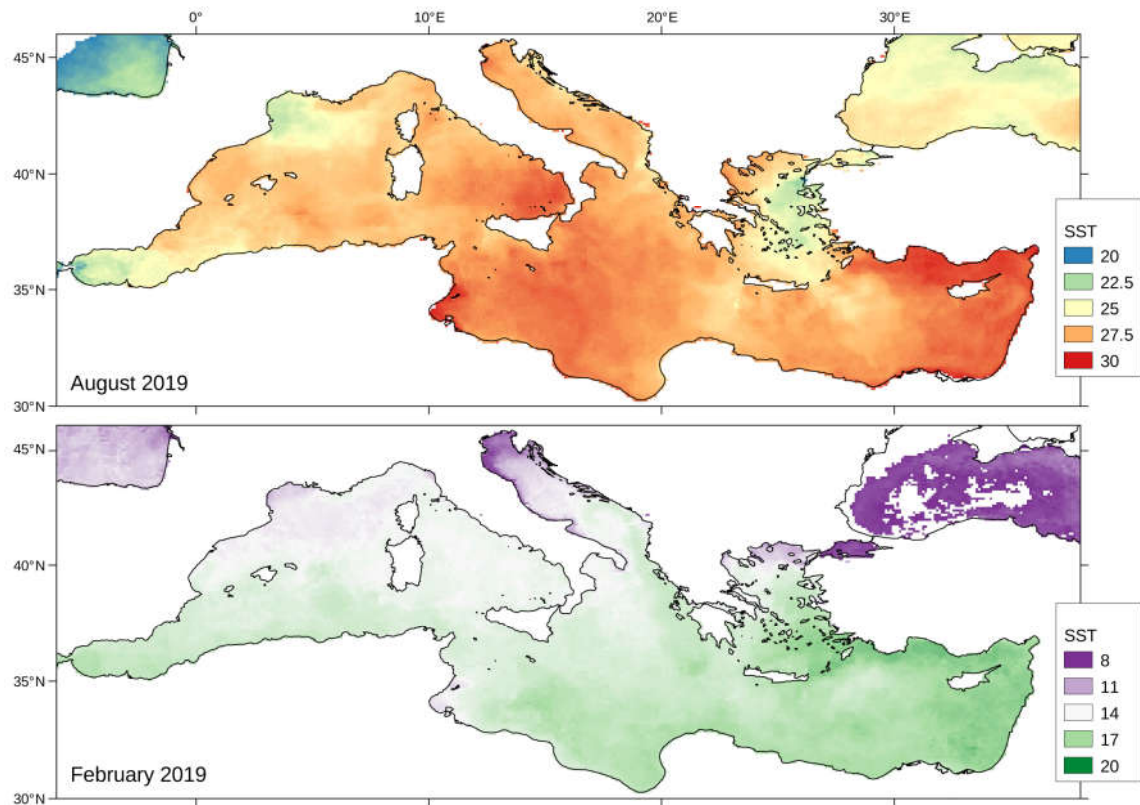
Fig. 11. Average SST of the Mediterranean. The data from MODIS (Moderate Resolution Imaging Spectroradiometer Satellite) represents two seasons in the Mediterranean: August, which is the warmest month and February, the coldest month. The east side of the Mediterranean is always warmer, which may explain the higher growth rates in the east relative to the west.

Tables

Table 1. New core elevations and ages from Israel. DRC refers to *Dendropoma*/Rock Contact and n.m. refers to "no measurements"

Location	Sp.	Sample	Elevation DGPS [m]	Sampling depth [cm]	$\delta^{13}C$ [‰ VPDB]	^{14}C ages yr. BP	Calib. BP [2σ]	Median	Calib. AD
Achziv S channel core 1	*V. triquetrus*	OxA-34573	0.44	DRC	2.0	868±25	324 - 520	422 [±98]	1528 [±98]
Achziv N channel core 3	*V. triquetrus*	OxA-34574	0.43	DRC	2.1	888±25	334 - 538	436 [±102]	1514 [±102]
Tel Dor N Bay Ramp	*V. triquetrus*	OxA-34575	0.18	DRC	0.75	595±21	48-277	163[±102]	1788[±102]
Minat A-ziv	Dendropoma sp.	MA-1	0.79	7	-0.8	480	< Cal range		
	Dendropoma sp.	MA-2	0.6	6	-0.7	495	< Cal range		

	Dendropoma sp.	MA-4	0.03	5	-0.9	470	< Cal range		
	Dendropoma sp.	MA-5	-0.27	7	-1.0	Modern			
Segavion Island	Dendropoma sp.	SI-1B (AC-1B)	n.m.	11.5	1.2	680±35	146-399	273	1677
	Dendropoma sp.	SI-2B (AC-2B)	n.m.	6	1.8	655±25	143-325	234	1716
	V. triquetrus	SI-3B (AC-3B)	n.m.	3	-0.5	Modern			
Akko	Dendropoma sp.	AK-4-B	-0.13	11	-0.3	Modern			

Table 2. Growth rates of the bio-constructions in specific sites across the Mediterranean surveyed in the current study. Calculations excluded short-cores who had 2 data points or less

Basin	Site			Growth rates
		name	code	mm yr^{-1}
West	Spain	Cabo de Gata, Playazo	CdG	0.09
		Punta Prima, Alicante	PPr	0.23
		Javea	Jav	0.08
		Avrg.		**0.13[±0.09]**
	Italy	Capo Gallo, Palermo – upper part	Gal	0.19
		Lower part		0.16
		Castelluzzo, S. VIto	Cas V1	0.18
		Cala Mancina, S. VIto	CMa V3	0.14
		Tonnara del Cofano, S. VIto	TDC	0.23
		Avrg.		**0.18[±0.03]**
	Tunisia	Sidi Mecrhig	SIM	0.11
East	Greece	Falasarna, Crete	Fal	1.0
	Israel	Shikmona - 1	Shik	1.04
		Shikmona - 2		1.22
		Atlit	Atl	1.08
		Hof Dor	HD	0.84
		Avrg.		**1.04[±0.15]**

Supplement Table 1: radiocarbon ages and depth data from drilled cores of *Dendropoma*, taken along a Mediterranean east-west transect, including Israel, Lebanon, Crete, Tunisia, Sicily and southern Spain. Previously published data, marked by the symbol [∗] are from Amitai et al., (2020).

	Site	Lab code	Drilling depth [cm]	δ¹³C [‰ VPDB]	¹⁴C activity [pMC]	¹⁴C Age [yr. BP]	Cal. Range [2σ cal. BP]	Cal. Age BP
Spain	∗Punta Prima Alicante,	PPr -30	3	0.2	106.3	Modern		
		PPr -54	54	0.9	98.6	120±30	< Cal range	
		PPr -100	10	0.0	93.5	540±20	1-228	115
		PPr -120	12	2.6	92.6	620±20	132-279	206
		PPr -130	13	-1.9	88.9	800±20	313-463	388
		PPr -140	14	-1.1	90.5	950±20	469-556	513
		PPr -175	17.5	-1.0	87.4	1080±30	540-662	601
		PPr -204	20.4	1.9	86.8	1140±20	612-710	661
	∗Cabo de Palos Playazo	CdGv4-53	5.3	4.8	94.9	425±30	< Cal range	
		CdGv4-110	11	3.7	93.5	540±25	1-228	115
		CdGv2-135	13.5	1.2	93.0	580±25	62-263	163
	∗Javea	Jav -50	5	-0.1	93.0	580±20	72-259	166
		Jav -80	8	0.7	90.3	820±20	329-479	404
		Jav -100	10	0.2	85.0	1300±20	725-885	805
		Jav -130	13	0.2	78.2	1980±20	1396-1555	1476
NW Sicily	∗Cala Mancina, S. VIto	CMA-v3-20	2	-1.8	107.4	Modern		
		CMA-v3-30	3	-0.6	94.9	420±20	< Cal range	
		CMA-v3-40	4	-1.0	93.5	540±20	1-228	115
		CMA-v3-50	5	3.7	93.5	540±20	1-228	115
		CMA-v3-60	6	5.1	92.8	600±20	108-271	190
		CMA-v3-80	8	4.2	90.4	810±20	320-472	396
		CMA-v3-100	10	3.7	85.8	1230±20	665-782	724
		CMA-v3-160	16	2.8	80.5	1740±20	1184-1300	1242
		CMA-v3-212	21.2	0.9	78.8	1915±25	1334-1508	1421
		CMA-v3-220c	22	2.7	78.7	1930±20	1354-1513	1434
		CMA-v3-260	26	-2.4	78.5	1950	1367-1531	1449
	∗Castelluzzo S. VIto,	CAS V1-40		0.56	101.1	Modern		
		CAS V1-50			97.4	210±20	< Cal range	
		CAS V1-60	6	4.5	93.2	570±35	48-260	154
		CAS V1-70	7		77.1	2085±45	1493-1743	1618
		CAS V1-125	12.5	2.5	75.8	2220±20	1693-1851	1772
		CAS V1-190	19	-4.3	72.7	2560±20	2106-2288	2197
		CAS V1-240	24	-1.8	70.2	2840±40	2382-2687	2535
	Capo Gallo, Palermo,	GAL-10	1	1.5	108.5	>Modern		
		GAL-15	1.5	-5.7	98.9	90±20	< Cal range	
		GAL-30	3		95.5	370±30	< Cal range	

		GAL-40	4	-4.7	93.3	560±20	51-249	150
		GAL-58	5.8		92.2	660±30	134-332	233
		GAL-70	7	0.1	91.0	760±20	290-428	359
		GAL-75	7.5	-1.6	90.7	790±20	307-455	381
		GAL-95	9.5	-5.8	78.1	1990±20	1402-1569	1486
		GAL-135	13.5		75.1	2300±30	1765-1961	1863
		GAL-194	19.4	-1.6	70.6	2790±20	2345-2595	2470
		GAL-267	26.7	-1.4	69.9	2880±20	2488-2697	2593
		GAL-323	32.3	-3.4	68.3	3060±20	2728-2848	2788
	Tonnara del Cofano S. VIto,	TDC-27	2.7	0.41	93.5	540±20	1-228	115
		TDC-36	0.6	0.68	92.8	600±20	108-271	190
		TDC-73	7.3	1.58	91.6	710±20	260-395	328
Tunisia	Les Grottes, El Haouaria	GRO-39	3.9	-1.5	109.0	>Modern		
		GRO-76	7.6	-4.5	96.8	264±22	< Cal range	
		GRO-127	12.7	-0.1	94.5	456±23	< Cal range	
		GRO-212	21.2	3.8	93.4	546±26	1-237	119
	*Sidi Mecrhig	SIM-60	6	-3.7	94.9	420±30	< Cal range	
		SIM-71	7.1	0.6	85.5	1260±30	674-855	765
		SIM-145	14.5	-1.5	80.1	1780±30	1222-1360	1291
Greece	Falasarna, Crete	Fal-43	4.3	-1.7	110.6	>Modern		
		Fal-55	5.5	-0.3	95.4	380±20	< Cal range	
		Fal-97	9.7	-4.0	93.9	500±20	1-134	68
		Fal-115	11.5	-0.3	93.9	500±20	1-134	68
		Fal-182	18.2	0.4	91.1	745±25	279-422	351
		Fal-230	23	-2.2	93.1	575±20	64-258	161
		Fal-280	28	-1.1	91.9	675±20	150-367	259
Lebanon	Batroun	BAT-41	4.1	-4.7	94.7	440±35	< Cal range	
		BAT-102	10.2	-3.4	76.4	2160±35	1585-1810	1698
	Tripoli	TRI-1 -39	3.9	-1.4	93.7	520±25	1-226	76
		TRI-1 -70	7	-4.9	93.9	505±25	1-147	74
		TRI-1 -119	11.9	-2.0	92.7	610±25	111-280	196
	Tyro	Tyr-F-7	0.7	-5.0	107.5	>Modern		
		Tyr-F-29	2.9	4.2	93.4	545±25	40-236	138
	Sidon	SID-2-20	2	1.1	114.7	>Modern		
		SID-2-35	3.5	0.8	94.6	445±30	< Cal range	
		SID-2-80	8	-0.1	90.3	815±30	315-480	398
		SID-2-109	11	-3.6	90.9	765±30	287-443	365
		SID-2-182	18.2	2.7	93.5	545±30	1-236	119
		SID-1-139	13.9	-1.7	93.7	520±30	1-150	76

607

608

609

610

611